



# Dynamic Nuclear Polarization enhanced NMR at 187 GHz/284 MHz using an Extended Interaction Klystron amplifier



Thomas F. Kemp<sup>a</sup>, Hugh R.W. Dannatt<sup>b</sup>, Nathan S. Barrow<sup>c</sup>, Anthony Watts<sup>b</sup>, Steven P. Brown<sup>a</sup>, Mark E. Newton<sup>a</sup>, Ray Dupree<sup>a,\*</sup>

<sup>a</sup> Department of Physics, University of Warwick, Coventry CV4 7AL, UK

<sup>b</sup> Department of Biochemistry, University of Oxford, OX1 3QU, UK

<sup>c</sup> Johnson Matthey Technology Centre, Blount's Court, Sonning Common, Reading RG4 9NH, UK

## ARTICLE INFO

### Article history:

Received 10 December 2015

Revised 15 January 2016

Available online 2 February 2016

### Keywords:

Dynamic Nuclear Polarisation

Quasi-optic microwaves

Extended Interaction Klystron amplifier

## ABSTRACT

A Dynamic Nuclear Polarisation (DNP) enhanced solid-state Magic Angle Spinning (MAS) NMR spectrometer which uses a 187 GHz (corresponding to <sup>1</sup>H NMR frequency of 284 MHz) Extended Interaction Klystron (EIK) amplifier as the microwave source is briefly described. Its performance is demonstrated for a biomolecule (bacteriorhodopsin), a pharmaceutical, and surface functionalised silica. The EIK is very compact and easily incorporated into an existing spectrometer. The bandwidth of the amplifier is sufficient that it obviates the need for a sweepable magnetic field, once set, for all commonly used radicals.

The variable power (CW or pulsed) output from the EIK is transmitted to the DNP-NMR probe using a quasi-optic system with a high power isolator and a corrugated waveguide which feeds the microwaves into the DNP-NMR probe. Curved mirrors inside the probe project the microwaves down the axis of the MAS rotor, giving a very efficient system such that maximum DNP enhancement is achieved with less than 3 W output from the microwave source. The DNP-NMR probe operates with a sample temperature down to 90 K whilst spinning at 8 kHz. Significant enhancements, in excess of 100 for bacteriorhodopsin in purple membrane (bR in PM), are shown along with spectra which are enhanced by  $\approx 25$  with respect to room temperature, for both the pharmaceutical furosemide and surface functionalised silica. These enhancements allow hitherto prohibitively time consuming experiments to be undertaken. The power at which the DNP enhancement in bR in PM saturates does not change significantly between 90 K and 170 K even though the enhancement drops by a factor of  $\approx 11$ . As the DNP build up time decreases by a factor 3 over this temperature range, the reduction in  $T_{1\rho}$  is presumably a significant contribution to the drop in enhancement.

© 2016 The Authors. Published by Elsevier Inc. This is an open access article under the CC BY license (<http://creativecommons.org/licenses/by/4.0/>).

## 1. Introduction

Magic Angle Spinning (MAS) NMR is widely used for obtaining structural and dynamic information about solids, however its use is often limited by sensitivity both because of the small nuclear magnetic moment and the fact that many experiments involve isotopes of low natural abundance. Dynamic Nuclear Polarisation (DNP) involves the transfer of the much larger thermal polarisation of electron spins to nearby nuclei by microwave irradiation at the appropriate frequency to induce electron-nuclear transitions and in principle could increase the sensitivity by the ratio of the electron and nuclear gyromagnetic moments  $\approx 660$  for <sup>1</sup>H. After the development of high frequency high power microwave sources [1], DNP began to be applied in contemporary NMR experiments

[2]. The subsequent development of commercial MAS DNP NMR spectrometers based on gyrotron sources [3] has led to rapid developments in both applications and theoretical understanding (for recent reviews see e.g. Lee et al. [4], Ni et al. [5], Rossini et al. [6] and Can et al. [7]). Most MAS DNP NMR experiments use nitroxide based radicals at between 100 and 110 K with a gyrotron microwave source. Whilst these sources perform well they require an additional superconducting magnet which must be located some distance from the NMR magnet so requiring significant extra space. Furthermore, the restricted tuning range of most gyrotrons means that the NMR magnet should ideally be sweepable to allow for the use of different radicals. Here we describe a MAS DNP spectrometer which uses a 187 GHz Extended Interaction Klystron (EIK) amplifier driven by a solid state multiplier chain as the microwave source. This corresponds to a <sup>1</sup>H NMR frequency of 283.7 MHz to suit our existing probes. The EIK has a bandwidth such that a

\* Corresponding author.

sweepable NMR magnet is not required, it can be simply added to an existing NMR spectrometer and pulsed and variable frequency experiments, whilst not described here, could be readily implemented. The irradiation of the sample is very efficient because the microwaves are projected down the axis of the MAS rotor as described previously [8]. The performance of the spectrometer is demonstrated for a biomolecular system, a pharmaceutical and a surface functionalised material.

## 2. Equipment description

The DNP NMR spectrometer is similar to that previously reported by Pike et al. [8] but with a tuneable 187 GHz Extended Interaction Klystron (EIK) amplifier as the microwave source, which obviates the need for the magnetic field to be varied once initially set, and a 7.05 T Oxford NMR magnet operating at 6.66 T ( $^1\text{H}$  frequency 283.7 MHz) with a Varian Infinity Plus console. The NMR probe is a modified triple channel MAS Doty DI-4 with extended VT capability which is able to spin stably at 8 kHz at 90 K for extended periods. The microwave system consists of a VDI Tx219 phase locked amplifier/multiplier chain having a maximum output of 71 mW feeding, via an isolator and a variable attenuator, a 187 GHz CPI EIK amplifier which has a maximum gain of 23.7 dB. The multiplier is driven either by an internal 11.700 GHz source or externally by an Agilent Technologies E8257C signal generator. The amplifier has a power output of up to 9 W with a 4 dB bandwidth of 0.41 GHz centred on 187.09 GHz. The microwaves are transmitted to the NMR probe via a quasi-optic transmission system similar to that described earlier [8] but optimised for 187 GHz. A ferrite rotator and polarising grids (Thomas Keating Ltd) act as a high power isolator to protect the EIK from any reflected power due to inadvertent poor coupling to the quasi-optic transmission system, the probe, or the sample itself. After the microwaves exit from the corrugated waveguide they pass through a PTFE window in the cryostat and are focussed by two mirrors onto the middle of the rotor cap where the beam waist (defined as  $1/e$  amplitude) diameter is approximately 1.2 mm (as described by Pike et al. [8]). The loss in the transmission system is estimated to be approximately 4 dB. The beam passes through the rotor cap and a Teflon spacer, both of which are hollow for most of their lengths, before reaching the sample. The beam waist at the top of the sample is expected to be comparable to the diameter of the rotor and, in addition, the silicon nitride rotor is likely to aid confinement of the microwave beam further improving the efficiency of the system. As in our earlier work [8], silver foil of thickness 0.5  $\mu\text{m}$  was attached to the top surface of the bottom spacer to increase the enhancement and to improve the uniformity of enhancement throughout the sample.

## 3. Samples

### 3.1. Urea with TOTAPOL or AMUPOL

The same sample (2 M  $^{13}\text{C}$  labelled urea (99%, Cambridge Isotope Laboratories Inc.) in glycerol- $d_8$ ,  $\text{D}_2\text{O}$  and  $\text{H}_2\text{O}$  (60:30:10 by volume) with 40 mM TOTAPOL) as in Pike et al. [8] was used for initial set-up. Most experiments were carried out with a lower concentration (10 mM TOTAPOL or 10 mM AMUPOL) of radical.

### 3.2. Bacteriorhodopsin in Purple Membrane (bR in PM)

$^2\text{H}$ -labelled (70%) and uniformly  $^{13}\text{C}$ ,  $^{15}\text{N}$ -labelled bacteriorhodopsin (bR) was expressed in *Halobacterium salinarum* strain S9 using rich labelled media and purified as purple membrane (PM) leaflets as described previously [9]. Isotopic labelling was

achieved by the use of appropriately labelled celtone media made up in 70%  $\text{D}_2\text{O}$ . After purification, 1.5 mg of labelled bR in PM was resuspended in 75  $\mu\text{l}$  of 20 mM sodium citrate buffer at pH 6.0 containing 15 mM AMUPOL [10] and 0.01% w/v  $\text{NaN}_3$ , made up with glycerol- $d_8$ ,  $\text{D}_2\text{O}$ ,  $\text{H}_2\text{O}$  at a ratio of 6:3:1. This sample was thoroughly mixed before being pipetted directly into a 4 mm rotor for DNP measurements.

### 3.3. Furosemide

Furosemide (100 mg) (supplied by AstraZeneca plc) was added to a pestle and mortar and ground for approximately 10 min until a talc like consistency was achieved. 60  $\mu\text{l}$  TEKPOL [11] solution (16 mM in 1,3 dibromobutane (98% Alfa Aesar)) was then added and ground for a further 5 min keeping the mixture moist by adding extra dibromobutane as required. The furosemide-TEKPOL mixture (101 mg) was then packed into a 4 mm rotor.

### 3.4. 3-Aminopropyl functionalised silica

Functionalised silica (Davisil G636, 60 Å pore size) was mixed with an excess of 5 mM TOTAPOL in  $\text{D}_2\text{O}:\text{H}_2\text{O}$  (90:10 *v:v*) solution and roughly mixed. This mixture was left for approximately 24 h at room temperature and was then centrifuged (12100g, 5 min) and excess TOTAPOL solution removed. The remaining damp powder was packed into a 4 mm rotor. Grinding the silica beforehand made no detectable difference to the enhancement achieved.

## 4. NMR

For all DNP experiments, microwave irradiation was applied during the recycle delay before the pulse sequence. CP experiments were performed with an 80% to 100% ramp [12] on the  $^1\text{H}$  channel and optimised contact times of between 0.6 ms and 1.5 ms were used. The  $^1\text{H}$  decoupling sequence used for all CP experiments was SPINAL-64 [13] with nutation frequency  $\nu_1 = 100$  kHz except for the  $^{13}\text{C}$  CP MAS of the furosemide sample where  $\nu_1 = 80$  kHz. The  $^{13}\text{C}$  spectra were referenced to the carbonyl peak at 177.8 ppm of L-alanine as an external reference with respect to TMS at 0 ppm. The  $^{15}\text{N}$  spectra were referenced using a known peak in the bR sample and is relative to liquid  $\text{NH}_3$  at  $-50^\circ\text{C}$ . The temperature was calibrated using the  $^{119}\text{Sn}$  shift of  $\text{Sm}_2\text{Sn}_2\text{O}_7$  as reported by Kemp et al. [14] from room temperature down to 86 K, and all experiments were carried out at 90 K and spinning at 8 kHz, unless otherwise stated.

Here enhancement,  $\varepsilon$ , is defined as  $\varepsilon = \frac{I - I_0}{I_0}$ , where  $I$  and  $I_0$  are the spectral intensities of the enhanced and unenhanced spectra respectively under identical conditions.

### 4.1. $^1\text{H}$ - $^{13}\text{C}$ HETCOR

A  $^1\text{H}$   $\nu_1$  nutation frequency of 100 kHz was used for the 90° pulse, PMLG [15] decoupling during mixing and TPPM [16] decoupling during acquisition. The contact time was 1 ms with a ramped  $^1\text{H}$   $\nu_1$  from 36 kHz to 40 kHz, and a constant  $^{13}\text{C}$   $\nu_1 \approx 52.5$  kHz. Microwave irradiation was applied during the 10 s recycle delay. 16 transients were co-added for each of the 64  $t_1$  slices with a spectral width in  $F_1$  of 5.36 kHz giving a total experimental time of 2 h 52 min. States-TPPI was used for sign discrimination in the indirect dimension.

### 4.2. $^{15}\text{N}$ - $^{13}\text{C}$ Double CP (DCP) HETCOR

The experiment is similar to that described by Baldus et al. [17] with the addition of DNP enhancement. Microwave irradiation is

applied for 1.5 s to transfer the electron polarisation to the hydrogen bath. A  $7.1 \mu\text{s}$   $90^\circ$  nitrogen preparation pulse is followed by  $^1\text{H}$  to  $^{15}\text{N}$  CP, a  $t_1$  period,  $^{15}\text{N}$  to  $^{13}\text{C}$  CP and then acquisition on  $^{13}\text{C}$ . The  $^1\text{H}$  to  $^{15}\text{N}$  CP sequence is a ( $\nu_1 = 100 \text{ kHz}$ )  $^1\text{H}$   $90^\circ$  pulse followed by a  $0.6 \text{ ms}$  ( $\nu_1 = 45 \text{ kHz}$ ) pulse on  $^1\text{H}$  together with a tan pulse [18] of central amplitude of  $35 \text{ kHz}$  on  $^{15}\text{N}$ . For  $^{15}\text{N}$  to  $^{13}\text{C}$  CP, the contact time was  $10 \text{ ms}$  with  $\nu_1 = 40 \text{ kHz}$  on  $^{15}\text{N}$  whilst the  $^{13}\text{C}$   $\nu_1$  is ramped from  $56 \text{ kHz}$  to  $43 \text{ kHz}$ . TPPM  $^1\text{H}$  decoupling of  $100 \text{ kHz}$  is applied during both the  $t_1$  period and acquisition with  $100 \text{ kHz}$  CW decoupling during the  $^{15}\text{N}$  to  $^{13}\text{C}$  CP transfer. 32 acquisitions per slice were acquired for a total of 98 slices and a  $t_1$  increment of  $282 \mu\text{s}$ . The signal had decayed by 40 slices ( $11.28 \text{ ms}$ ) giving an experimental time (with 40 slices) of 32 min or 78 min for the complete experiment. TPPI was used for sign discrimination in the indirect dimension.

## 5. Results

In any DNP set up it is first necessary to determine the optimum frequency for DNP since the enhancement varies as a function of irradiation position within the EPR spectrum. This was done using the 2 M urea with 40 mM TOTAPOL sample from Pike et al. [8]. Normally the NMR magnetic field is swept to find the optimum frequency, but in our case the field is fixed and the frequency varied. The frequency dependence of signal enhancement for this sample is shown in Fig. 1. The maximum enhancement of approximately +80 is at  $187.0 \text{ GHz}$ . The shape roughly follows the first derivative of the ESR lineshape, is asymmetric with the maximum negative enhancement being approximately 75% of the positive value, and the separation between the maximum positive and negative enhancements is  $0.14 \text{ GHz}$ . The 4 dB points of the ELK (minimum of  $3.5 \text{ W}$  between  $186.88 \text{ GHz}$  and  $187.29 \text{ GHz}$ ) cover both the positive and negative peaks of the enhancement curve and also give sufficient range to adjust the frequency for any similar radical. For the experimental data presented subsequently the frequency corresponding to the positive maximum enhancement was employed. Of the radicals tested so far TOTAPOL, AMUPOL and TEKPOL give maximum enhancements at very similar frequencies, and we did not find any changes necessary, however future radicals are likely to require some adjustments in irradiation frequency depending on the  $g$  value and the nature of the radical.

Fig. 2 shows the  $^{13}\text{C}$  enhancement achieved for the partially deuterated bacteriorhodopsin sample at  $90 \text{ K}$  using  $15 \text{ mM}$  AMUPOL as the radical. Both the  $^{13}\text{C}$  and  $^{15}\text{N}$  (shown in Fig. S11)

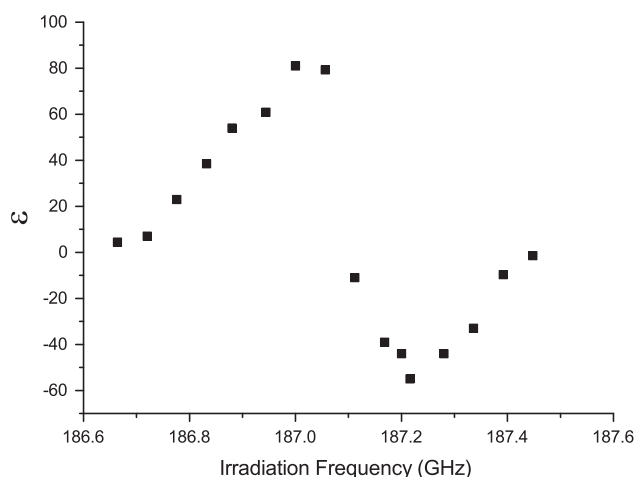


Fig. 1.  $^1\text{H}$  DNP enhancement ( $^{13}\text{C}$  Detected) for 2 M Urea in glycerol- $d_8$ ,  $\text{D}_2\text{O}$  and  $\text{H}_2\text{O}$  with 40 mM TOTAPOL as a function of irradiation frequency at  $6.66 \text{ T}$ .

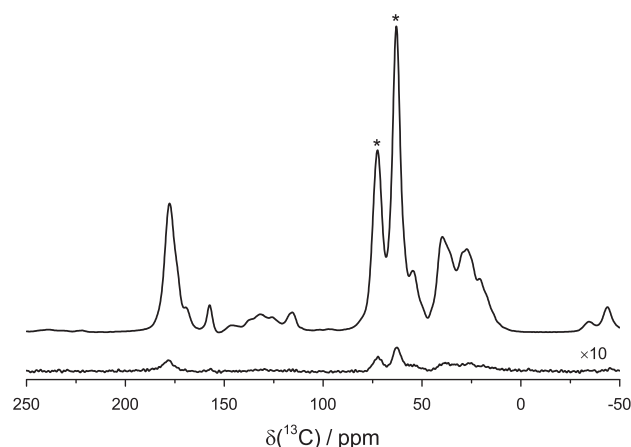
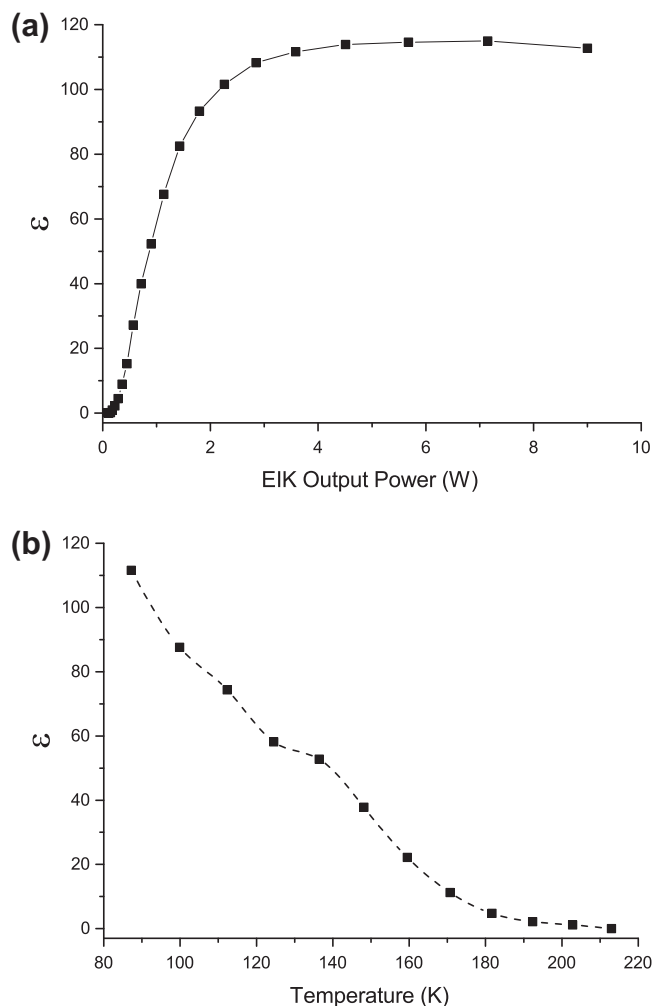


Fig. 2.  $^1\text{H}$ - $^{13}\text{C}$  CP DNP spectra of bacteriorhodopsin in purple membrane using AMUPOL radical at  $90 \text{ K}$ . The unenhanced spectrum (lower) has been multiplied by 10 to allow better comparison. The two stars (\*) denote glycerol peaks from the buffer. Both spectra were acquired with 256 co-added transients and a  $3 \text{ s}$  recycle delay. The enhancement achieved is approximately 120.

enhancements are approximately 120, although the  $^{15}\text{N}$  enhancement is somewhat less certain due to the poor signal to noise ratio in the unenhanced spectrum, even after approximately one hour of averaging. Notably, the microwave power is not the limiting factor in the performance of the spectrometer since the enhancement saturates at a source power level of approximately  $3 \text{ W}$  (Fig. 3a) corresponding to, at most,  $1.5 \text{ W}$  at the rotor top. This is in contrast to systems which couple the microwave power to the sample through the rotor walls where the enhancement at  $80 \text{ K}$  did not saturate at their maximum power of  $12.5 \text{ W}$ , see Ni et al. [5]. Furthermore the enhancement does not reduce with increased power indicating that sample heating is minimal even with  $9 \text{ W}$  of microwave source power (Fig. 3a). As an additional check for sample heating, a split KBr powder and water/glycerol sample was made and the minimal changes in  $^{79}\text{Br}$  shift [19] showed that any change in temperature with increased microwave power was less than  $5 \text{ K}$ .

There have been a number of simulations of the enhancement due to the Cross Effect for example by Thurber and Tycko [20], Mentink-Vigier et al. [21,22], Mance et al. [23]. In the simulations by Thurber and Tycko [20], it was found that, after initially increasing rapidly with the microwave nutation frequency,  $\nu_{1e}$ , the nuclear spin polarisation becomes approximately constant at nutation frequencies of between  $0.5 \text{ MHz}$  and  $1.0 \text{ MHz}$  as the electron spin lattice relaxation time,  $T_{1e}$ , changes from  $2 \text{ ms}$  to  $0.2 \text{ ms}$ . The very recent simulation of Mentink-Vigier et al. [22] also found that, for a  $T_{1e}$  of  $1 \text{ ms}$ , the enhancement was only weakly dependent on rf amplitude for nutation frequencies above  $\sim 1.0 \text{ MHz}$  indicating that  $\nu_{1e}$  in our system reaches values in this range for an ELK output power of  $2 \text{ W}$  to  $3 \text{ W}$ . The resolution of the bR spectrum is significantly worse than at room temperature at  $800 \text{ MHz}$  for a sample with no radical, particularly in the aliphatic region. As the broadening of the lines is due to the molecular motion being much reduced at  $90 \text{ K}$ , as well as possibly the presence of the paramagnetic radical, the temperature dependence of the enhancement was measured (Fig. 3b). Although the enhancement decreases quite rapidly with increasing temperature it is still greater than 10 at  $170 \text{ K}$ . Also the build-up time,  $T_{1b}$ , (shown in Fig. S12) becomes significantly shorter at higher temperatures, decreasing by a factor  $\approx 3$  from  $\approx 1.5 \text{ s}$  at  $90 \text{ K}$  to  $\approx 0.5 \text{ s}$  at  $170 \text{ K}$  which enables data to be acquired more rapidly.

The effect of microwave power on enhancement was also determined at  $170 \text{ K}$  and somewhat surprisingly the behaviour was very similar to that at  $90 \text{ K}$ , i.e., the power needed for maximum



**Fig. 3.** (a)  $^1\text{H}$  ( $^{13}\text{C}$  Detected) enhancement as a function of EIK output power for the bacteriorhodopsin sample using AMUPOL radical at 90 K. (b)  $^1\text{H}$  ( $^{13}\text{C}$  Detected) enhancement of the same sample as a function of temperature. Experiments were performed with a recycle delay of  $5 \times T_{1B}$  and sufficient acquisitions (up to 128) to achieve a signal to noise ratio of greater than 20:1 in the unenhanced signal.

enhancement remained the same (shown in Fig. S13) even though the enhancement had dropped by a factor  $\approx 11$ . Since  $T_{1B}$  decreased by a factor  $\approx 3$  in going from 90 K to 170 K, it would seem that a significant contribution to the reduction in enhancement in this case is the reduction in  $T_{1n}$ . The nuclear spins have a range of distances from the polarising agent and a shorter  $T_{1n}$  will reduce the time for the polarisation to diffuse through the sample and thus the effective sample volume.

With the increased sensitivity for the bR sample, a 2D DCP HET-COR experiment could be run at 90 K in less than 1 h (on an undeuterated sample where the enhancement in the 1D spectrum was approximately 50) compared with 30 h at room temperature and with the sensitivity advantage of a higher field (800 MHz) (shown in Fig. S14). However, as found elsewhere (see Koers et al. [24] for a recent discussion) the resolution is much worse than at room temperature. Nevertheless the rapid acquisition of the HET-COR spectrum indicates that DNP could be useful for selectively labelled samples. Interestingly the decreased molecular motion at low temperature brings up a new peak, centred on  $\delta = 32$  ppm ( $^{13}\text{C}$ ),  $\delta = 121$  ppm ( $^{15}\text{N}$ ), most likely from amino acid side chains in the protein which contain N–C pairs. The experiment was repeated at 170 K, where a full 2D spectrum could be obtained in about 4 h. The resolution was higher and the carbon peak around

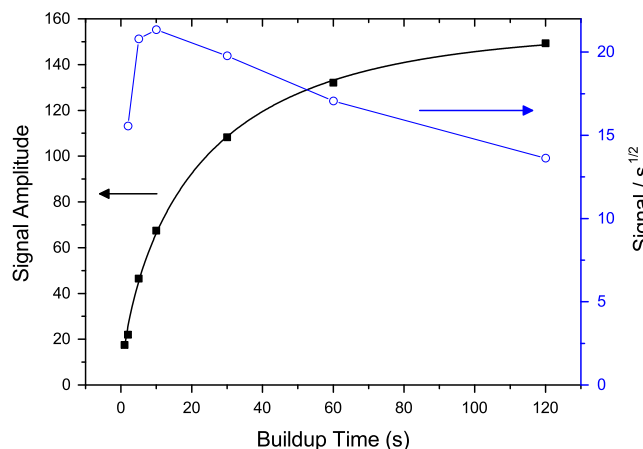


**Fig. 4.**  $^{13}\text{C}$  signal build-up of furosemide with 16 mM TEKPOL in dibromobutane, squares. The signal amplitude has been fitted to a stretched exponential with a  $T_{1B}$  of 23 s and a stretching factor  $\beta$  of 0.70. The circles show the signal per root second which is optimal for a build-up time of  $\sim 10$  s.

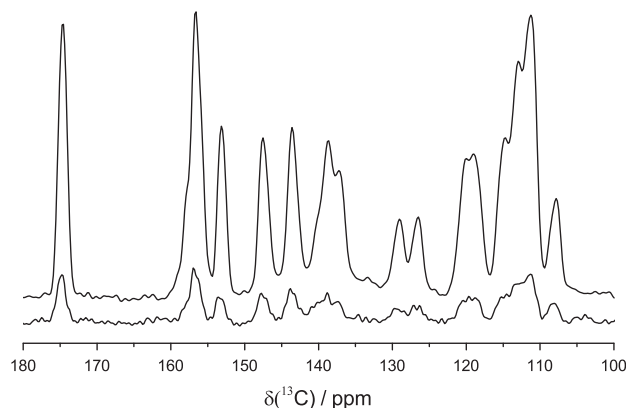


**Fig. 5.**  $^{13}\text{C}$  CP MAS Spectra of furosemide using 16 mM TEKPOL in dibromobutane as the polarising agent. 64 acquisitions with a 10 s build-up delay were acquired. The top spectrum is DNP enhanced. The enhancement achieved with this build-up time was approximately 5.5.

$\delta = 32$  ppm was no longer visible indicating that there are significant dynamics in the system at this temperature, however the resolution was not high enough to be useful for subsequent NMR analysis.

The pharmaceutical furosemide has a long  $T_{1n}$  ( $^1\text{H}$ ) at room temperature ( $\approx 25$  s) making 2D experiments very time consuming or infeasible. The DNP build up curve for the furosemide with radical, shown in Fig. 4, fits well to a stretched exponential,  $A = A_0(1 - e^{-(t/T_{1B})^\beta})$ , where  $\beta$  is the stretching factor (0.70 in this case), indicative of a wide range of environments. The distribution in particle size results in a distribution of  $T_{1B}$  values as the radical is further from some parts of the sample than others. As a consequence a similar S/N per unit time, also shown in Fig. 4, is obtained for build-up times between 5 s and 30 s. As suggested by Rossini et al. [25] the particle size distribution could be measured by comparing the signal build up with and without DNP. However this would be very time consuming in this case due to the long  $T_{1n}$  of the bulk sample and the weak signal without DNP enhancement. Fig. 5 shows that the  $^{13}\text{C}$  enhancement obtained is approximately  $\epsilon = 5.5$  using a build-up time of 10 s. The effective improvement obtained by using DNP is given not just by the enhancement  $\epsilon$  but also by the Boltzmann factor and reduced noise in the coil, commonly taken as 3.6 [26], and the ability to pulse more rapidly



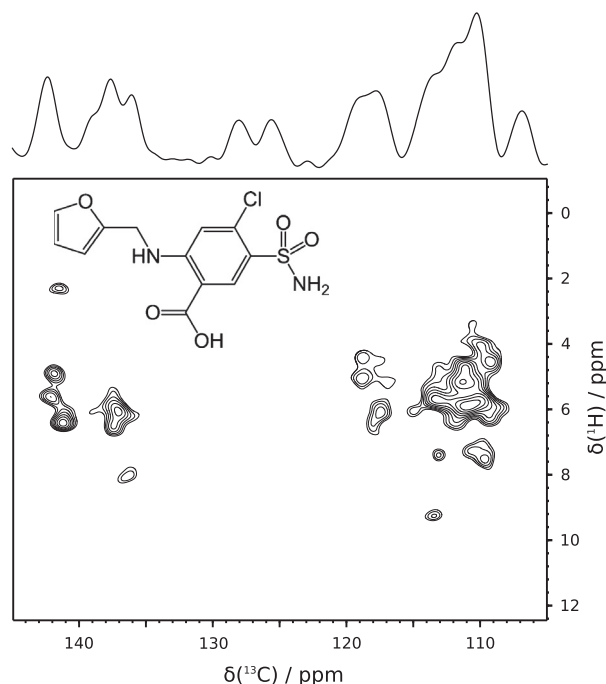


**Fig. 6.**  $^{13}\text{C}$ - $^1\text{H}$  HETCOR of furosemide, mixing time 1 ms, using TEKPOL in dibromobutane. 64 slices were acquired with a spectral width in the indirect dimension,  $F_1$ , of 5.36 kHz and 16 acquisitions per slice using a build-up delay of 10 s. The total run time was 2 h 52 min. The 1D spectrum is shown above.

if the  $T_1$  is reduced. However, as this sample had a large distribution of particle sizes and hence range of DNP build up times, although it is possible to pulse faster there is little extra gain in sensitivity and the total improvement is approximately 25, since the amount of sample and linewidths are almost unchanged. Comparison with the room temperature spectrum (see Fig. S15) shows that the broad feature extending from  $\sim 127$  ppm to 129 ppm has split into 2 peaks at 90 K and the relative intensities of the overlapping peaks around 111 ppm has changed. Changes of similar magnitude between room temperature and 100 K have been observed

by Pinon et al. [27] in the spectra of various polymorphs of the pharmaceutical theophylline and by Marker et al. [28] in a 2'-deoxyguanosine derivative. To illustrate the gain in sensitivity, a 2D  $^1\text{H}$ - $^{13}\text{C}$  HETCOR experiment with a mixing time of 1 ms was undertaken. This spectrum (Fig. 6) was obtained in under 3 h, whereas a  $J$ -coupled HETCOR experiment taken on a 500 MHz spectrometer (spectrum not shown) took 5 days to give a similar spectrum.

To show the application of DNP to surface enhancement of a material, a 3-aminopropyl functionalised silica sample was studied using incipient wetness to distribute the TOTAPOL radical around the surface. The  $^{13}\text{C}$  build-up for this sample is also best described by a stretched exponential (see Fig. S16), although in this case  $\beta = 0.85$  is much closer to 1 (meaning a single exponential) than the furosemide sample ( $\beta = 0.70$ ) indicating a smaller range of environments and/or distribution of radical distance from the surface. This is unsurprising given that the carbon being detected was exclusively at the surface, rather than throughout the bulk. However, it does indicate that the radical was not uniformly distributed with respect to the functionalised material. Optimum build-up times were around 4–10 s. Fig. 7 shows the  $^{13}\text{C}$  spectrum with and without microwave irradiation for a recycle time of 6 s, which gave  $\varepsilon = 6.7$ . The  $^{15}\text{N}$  spectrum of this sample could be obtained in approximately 1 h of acquisition using DNP at 90 K (inset in Fig. 7) together with a room temperature spectrum which took 20 h of acquisition. The effective enhancement achieved was  $\varepsilon = 25$  as the amount of sample and linewidths are unchanged. As DNP offers over a factor 600 time saving for acquiring natural abundance  $^{15}\text{N}$  spectra of functionalised silica, DNP enables an otherwise prohibitive characterisation method to become routine.

## 6. Conclusion

A DNP NMR system based on an EIK microwave amplifier has been described that has significantly demonstrated and potential advantages over gyrotron based systems. No additional superconducting magnet is required reducing space requirements, running and capital costs. The bandwidth of the amplifier allows easy change of frequency, sufficient to cover existing nitroxide based radicals without a change of magnetic field, and which is likely

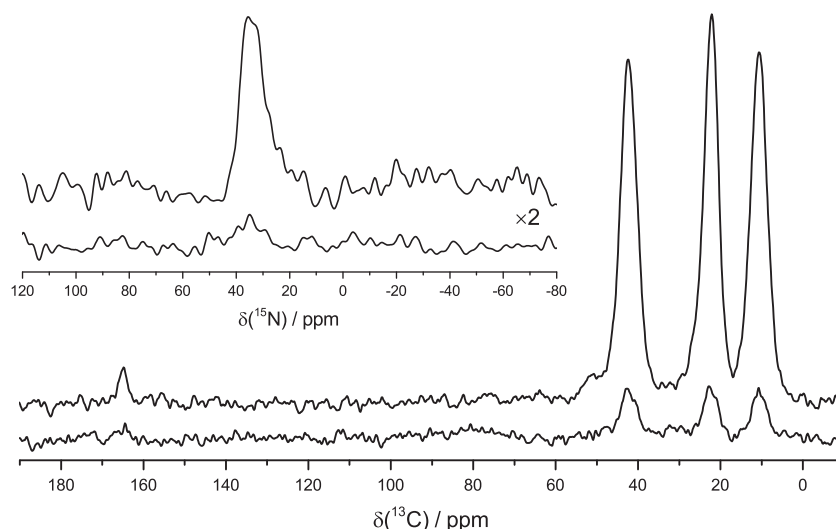


**Fig. 7.**  $^{13}\text{C}$  CP MAS spectra of 3-aminopropyl functionalised silica using 5 mM TOTAPOL as the polarising agent.  $\varepsilon = 6.7$ . Both  $^{13}\text{C}$  spectra were acquired with 64 acquisitions and 6 s recycle time, the upper spectrum is DNP enhanced. The inset shows  $^{15}\text{N}$  CP spectra of the same sample. The upper, DNP enhanced, spectrum was acquired at 90 K with a 6 s build-up delay for approximately 1.1 h. The lower spectrum was acquired at room temperature with a recycle delay of 3 s ( $5 \times T_1$  for an undoped sample) for 20.5 h. The spectra have been normalised to the same experimental time. The enhancement achieved relative to room temperature is approximately 25.

to be of use when developing new polarisation radicals. It also allows the possibility of frequency modulation [29] and pulsed DNP experiments to be undertaken, with such developments ongoing in our laboratory. The EIK is particularly easy to use, is very compact and can be readily incorporated into existing NMR systems. As previously demonstrated [8], the quasi-optic system, which projects a focussed beam of microwaves down the axis of the MAS rotor, together with the silver foil on the bottom rotor cap is very efficient and can be easily modified to increase functionality of the system. Due to the high efficiency of the quasi-optic system significantly lower microwave power (less than 3 W) is required than hitherto published for full DNP enhancement.

Significant DNP enhancements have been achieved in a wide range of samples with different radicals. For bacteriorhodopsin in purple membrane using AMUPOL radical, the enhancement was  $\varepsilon = 120$  at 90 K and was still greater than  $\varepsilon = 10$  at 170 K. However, as demonstrated elsewhere [7,24] the decreased molecular motion at low temperature meant that there was considerable spectral broadening. Interestingly, features that were not visible at room temperature appear in the 2D spectrum at 90 K. For furosemide and for functionalised silica the enhancements were smaller, being about 25 compared with room temperature. Nevertheless this is sufficient to allow 2D experiments to be undertaken in a reasonable time and previously impracticable  $^{15}\text{N}$  data to be obtained. In conclusion, our work demonstrates that an existing conventional solid-state NMR system can be adapted to run DNP experiments via the use of an EIK microwave amplifier.

## Acknowledgments

Partial support for this work was provided by EPSRC (U.K.) (EP/K011944/1). We thank the ILL Deuteration Laboratory for deuteration and labelling of the purple membrane under JRA7 consortium contract HPR1-2001-50065 and R113-CT-2003-505925. Dr. Ouari is thanked for the TEKPOL and AMUPOL and Dr. Les Hughes from Astra Zeneca plc for the furosemide. The experimental data sets for this study are provided as a supporting dataset from WRAP, the Warwick Research Archive Portal at <http://wrap.warwick.ac.uk/76111>.

## Appendix A. Supplementary material

Supplementary data associated with this article can be found, in the online version, at <http://dx.doi.org/10.1016/j.jmr.2016.01.021>.

## References

- [1] L.R. Becerra, G.J. Gerfen, R.J. Temkin, D.J. Singel, R.G. Griffin, Dynamic nuclear polarization with a cyclotron resonance maser at 5 T, *Phys. Rev. Lett.* 71 (1993) 3561–3564, <http://dx.doi.org/10.1103/PhysRevLett.71.3561>.
- [2] G.J. Gerfen, L.R. Becerra, D.A. Hall, R.G. Griffin, R.J. Temkin, D.J. Singel, High frequency (140 GHz) dynamic nuclear polarization: polarization transfer to a solute in frozen aqueous solution, *J. Chem. Phys.* 102 (1995) 9494–9497, <http://dx.doi.org/10.1063/1.468818>.
- [3] M. Rosay, L. Tometich, S. Pawsey, R. Bader, R. Schauwecker, M. Blank, et al., Solid-state dynamic nuclear polarization at 263 GHz: spectrometer design and experimental results, *Phys. Chem. Chem. Phys.* 12 (2010) 5850–5860, <http://dx.doi.org/10.1039/c003685b>.
- [4] D. Lee, S. Hediger, G. De Paëpe, Is solid-state NMR enhanced by dynamic nuclear polarization?, *Solid State Nucl. Magn. Reson.* 66–67 (2015) 6–20, <http://dx.doi.org/10.1016/j.ssnmr.2015.01.003>.
- [5] Q.Z. Ni, E. Daviso, T.V. Can, E. Markhasin, S.K. Jawa, T.M. Swager, et al., High frequency dynamic nuclear polarization, *Acc. Chem. Res.* 46 (2013) 1933–1941, <http://dx.doi.org/10.1021/ar300348n>.
- [6] A.J. Rossini, A. Zagdoun, M. Lelli, A. Lesage, C. Copéret, L. Emsley, Dynamic nuclear polarization surface enhanced NMR spectroscopy, *Acc. Chem. Res.* 46 (2013) 1942–1951, <http://dx.doi.org/10.1021/ar300322x>.
- [7] T.V. Can, Q.Z. Ni, R.G. Griffin, Mechanisms of dynamic nuclear polarization in insulating solids, *J. Magn. Reson.* 253 (2015) 23–35, <http://dx.doi.org/10.1016/j.jmr.2015.02.005>.
- [8] K.J. Pike, T.F. Kemp, H. Takahashi, R. Day, A.P. Howes, E.V. Kryukov, et al., A spectrometer designed for 6.7 and 14.1 T DNP-enhanced solid-state MAS NMR using quasi-optical microwave transmission, *J. Magn. Reson.* 215 (2012) 1–9, <http://dx.doi.org/10.1016/j.jmr.2011.12.006>.
- [9] H.R.W. Dannatt, G.F. Taylor, K. Varga, V.A. Higman, M.-P. Pfeil, L. Asilmovska, et al.,  $^{13}\text{C}$ - and  $^1\text{H}$ -detection under fast MAS for the study of poorly available proteins: application to sub-milligram quantities of a 7 trans-membrane protein, *J. Biomol. NMR* 62 (2015) 17–23, <http://dx.doi.org/10.1007/s10858-015-9911-1>.
- [10] C. Sauvé, M. Rosay, G. Casano, F. Aussenac, R.T. Weber, O. Ouari, et al., Highly efficient, water-soluble polarizing agents for dynamic nuclear polarization at high frequency, *Angew. Chemie Int. Ed.* 52 (2013) 10858–10861, <http://dx.doi.org/10.1002/anie.201304657>.
- [11] A. Zagdoun, G. Casano, O. Ouari, M. Schwarzwälder, A.J. Rossini, F. Aussenac, et al., Large molecular weight nitroxide biradicals providing efficient dynamic nuclear polarization at temperatures up to 200 K, *J. Am. Chem. Soc.* 135 (2013) 12790–12797, <http://dx.doi.org/10.1021/ja405813t>.
- [12] G. Metz, X.L. Wu, S.O. Smith, Ramped-amplitude cross polarization in magic-angle-spinning NMR, *J. Magn. Reson. Ser. A* 110 (1994) 219–227, <http://dx.doi.org/10.1006/jmra.1994.1208>.
- [13] B.M. Fung, A.K. Khitrin, K. Ermolaev, An improved broadband decoupling sequence for liquid crystals and solids, *J. Magn. Reson.* 142 (2000) 97–101, <http://dx.doi.org/10.1006/jmre.1999.1896>.
- [14] T.F. Kemp, G. Balakrishnan, K.J. Pike, M.E. Smith, R. Dupree, Thermometers for low temperature Magic Angle Spinning NMR, *J. Magn. Reson.* 204 (2010) 169–172, <http://dx.doi.org/10.1016/j.jmr.2010.02.018>.
- [15] E. Vinogradov, P.K. Madhu, S. Vega, High-resolution proton solid-state NMR spectroscopy by phase-modulated Lee-Goldburg experiment, *Chem. Phys. Lett.* 314 (1999) 443–450, [http://dx.doi.org/10.1016/S0009-2614\(99\)01174-4](http://dx.doi.org/10.1016/S0009-2614(99)01174-4).
- [16] A.E. Bennett, C.M. Rienstra, M. Auger, K.V. Lakshmi, R.G. Griffin, Heteronuclear decoupling in rotating solids, *J. Chem. Phys.* 103 (1995) 6951, <http://dx.doi.org/10.1063/1.470372>.
- [17] M. Baldus, D.G. Geurts, S. Hediger, B.H. Meier, Efficient  $^{15}\text{N}$ - $^{13}\text{C}$  polarization transfer by adiabatic-passage Hartmann-Hahn cross polarization, *J. Magn. Reson. Ser. A* 118 (1996) 140–144, <http://dx.doi.org/10.1006/jmra.1996.0022>.
- [18] S. Hediger, B.H. Meier, R.R. Ernst, Adiabatic passage Hartmann-Hahn cross polarization in NMR under magic angle sample spinning, *Chem. Phys. Lett.* 240 (1995) 449–456, [http://dx.doi.org/10.1016/0009-2614\(95\)00505-X](http://dx.doi.org/10.1016/0009-2614(95)00505-X).
- [19] K.R. Thurber, R. Tycko, Measurement of sample temperatures under magic-angle spinning from the chemical shift and spin-lattice relaxation rate of  $^{79}\text{Br}$  in KBr powder, *J. Magn. Reson.* 196 (2009) 84–87, <http://dx.doi.org/10.1016/j.jmr.2008.09.019>.
- [20] K.R. Thurber, R. Tycko, Theory for cross effect dynamic nuclear polarization under magic-angle spinning in solid state nuclear magnetic resonance: the importance of level crossings, *J. Chem. Phys.* 137 (2012) 084508, <http://dx.doi.org/10.1063/1.4747449>.
- [21] F. Mentink-Vigier, Ü. Akbey, Y. Hovav, S. Vega, H. Oschkinat, A. Feintuch, Fast passage dynamic nuclear polarization on rotating solids, *J. Magn. Reson.* 224 (2012) 13–21, <http://dx.doi.org/10.1016/j.jmr.2012.08.013>.
- [22] F. Mentink-Vigier, Ü. Akbey, H. Oschkinat, S. Vega, A. Feintuch, Theoretical aspects of magic angle spinning – dynamic nuclear polarization, *J. Magn. Reson.* 258 (2015) 102–120, <http://dx.doi.org/10.1016/j.jmr.2015.07.001>.
- [23] D. Mance, P. Gast, M. Huber, M. Baldus, K.L. Ivanov, The magnetic field dependence of cross-effect dynamic nuclear polarization under magic angle spinning, *J. Chem. Phys.* 142 (2015) 234201, <http://dx.doi.org/10.1063/1.4922219>.
- [24] E.J. Koers, E.A.W. van der Cruysen, M. Rosay, M. Weingarth, A. Prokofyev, C. Sauvé, et al., NMR-based structural biology enhanced by dynamic nuclear polarization at high magnetic field, *J. Biomol. NMR* 60 (2014) 157–168, <http://dx.doi.org/10.1007/s10858-014-9865-8>.
- [25] A.J. Rossini, C.M. Widdifield, A. Zagdoun, M. Lelli, M. Schwarzwälder, C. Copéret, et al., Dynamic nuclear polarization enhanced NMR spectroscopy for pharmaceutical formulations, *J. Am. Chem. Soc.* 136 (2014) 2324–2334, <http://dx.doi.org/10.1021/ja4092038>.
- [26] H. Takahashi, D. Lee, L. Dubois, M. Bardet, S. Hediger, G. De Paëpe, Rapid natural-abundance 2D  $^{13}\text{C}$ - $^{13}\text{C}$  correlation spectroscopy using dynamic nuclear polarization enhanced solid-state NMR and matrix-free sample preparation, *Angew. Chemie Int. Ed.* 51 (2012) 11766–11769, <http://dx.doi.org/10.1002/anie.201206102>.
- [27] A.C. Pinon, A.J. Rossini, C.M. Widdifield, D. Gajan, L. Emsley, Polymorphs of theophylline characterized by DNP enhanced solid-state NMR, *Mol. Pharm.* 12 (2015) 4146–4153, <http://dx.doi.org/10.1021/acs.molpharmaceut.5b00610>.
- [28] K. Märker, M. Pingret, J.-M. Mouesca, D. Gasparutto, S. Hediger, G. De Paëpe, A new tool for NMR crystallography: complete  $^{13}\text{C}/^{15}\text{N}$  assignment of organic molecules at natural isotopic abundance using DNP-enhanced solid-state NMR, *J. Am. Chem. Soc.* 137 (2015) 13796–13799, <http://dx.doi.org/10.1021/jacs.5b09964>.
- [29] Y. Hovav, A. Feintuch, S. Vega, D. Goldfarb, Dynamic nuclear polarization using frequency modulation at 3.34 T, *J. Magn. Reson.* 238 (2014) 94–105, <http://dx.doi.org/10.1016/j.jmr.2013.10.025>.